

Tests of the JEF-2 $^{238}\text{U} + \text{n}$ Evaluation in the Unresolved Resonance Region

F.H. Fröhner
Kernforschungszentrum Karlsruhe
Institut für Neutronenphysik und Reaktortechnik
Postfach 3640, W-7500 Karlsruhe 1
Germany

ABSTRACT. During the JEF-2 test phase the new evaluation for $^{238}\text{U} + \text{n}$ in the unresolved resonance region has been checked against recent capture cross section measurements and against thick-sample transmission data and capture self-indication ratios. Effects of the unresolved resonance structure on self-shielding and multiple scattering were treated by Monte Carlo techniques based on resonance statistics and average resonance parameters. It was found that the average cross sections and average resonance parameters given in the new evaluation permit very satisfactory reproduction of all the measurements used in the tests.

1. Introduction

At present the cross section resonances of $^{238}\text{U} + \text{n}$ have been resolved and analysed up to 10 keV (Moxon et al. 1989). The resonance structure of the ^{238}U neutron cross sections persists, of course, also above 10 keV but resonance overlap increases and instrumental resolution deteriorates with growing neutron energy. The resonance structure at higher energies is therefore unresolved or at best partially resolved in the available experimental data. Now any resonance structure, whether resolved or not, causes phenomena such as resonance self-shielding and temperature-dependent resonance absorption, effects that are not only essential for the correct extraction of average total and capture cross sections from experimental resonance-averaged transmission and capture yield data, but also crucial for questions of reactor safety, e. g. about the temperature dependence of the reactivity (Doppler coefficient). The effects of unobserved resonances become unimportant only above roughly 150 to 200 keV for ^{238}U .

Modern evaluated nuclear data files contain, therefore, not only average point cross sections for the unresolved resonance region but also average resonance parameters characterising the resonance structure. In a recent ENDF6-formatted evaluation of $^{238}\text{U} + \text{n}$ (Fröhner 1989) the unresolved resonance region was taken to extend from 10 keV to 300 keV. This evaluation was adopted up to 200 keV for JEF-2, up to 149 keV for ENDF/B-VI, so that between 10 keV and 149 keV the point cross sections in JEF-2 and ENDF/B-VI are practically the same. During the test phase of JEF-2 a number of checks against experimental data were performed: (i) The JEF-2 point data were compared with new capture data, (ii) Monte Carlo calculations based on the JEF-2 average resonance parameters were

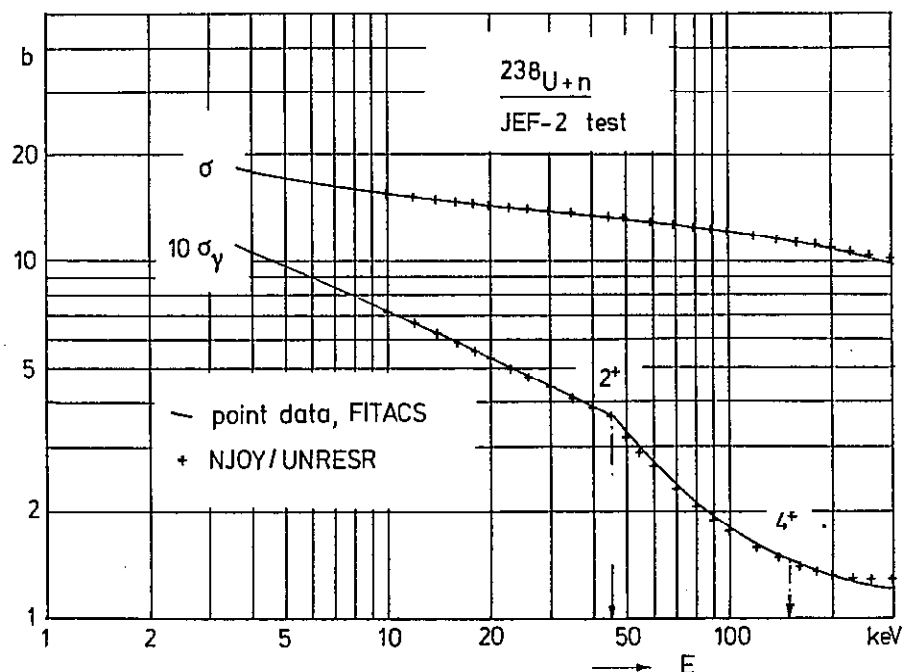


Fig. 1. Comparison of recommended average total and capture cross sections (curves, through JEF-2 point data) with cross sections (crosses) calculated with the NJOY Nuclear Data Processing System from the average resonance parameters given in JEF-2 for self-shielding calculations.

performed in order to find out how well they reproduce the comprehensive data base of measured thick-sample transmission values and capture self-indication ratios. The results of the comparisons are reported below, but it is appropriate to discuss first the consistency of the point data and average resonance parameters given in the new ^{238}U file.

2. Consistency Between Evaluated Average Cross Sections and Average Resonance Parameters.

If point cross sections are given together with average resonance parameters, as in the new evaluation of the unresolved region of $^{238}\text{U} + n$, there is always the question of consistency between the two. In the present case the evaluated point cross sections were generated by a cross section fitting program (FITACS, see Fröhner 1989) which uses Hauser-Feshbach theory in a form that is more sophisticated than the single-level Breit-Wigner treatment allowed by current ENDF rules for the unresolved resonance region, and implemented in processing codes for ENDF-formatted evaluated files. Differences exist, for instance, with respect to the treatment of width fluctuation corrections, the use of effective nuclear radii, and the number of inelastic channels admitted. It is therefore not to be expected that ENDF-type processing codes such as NJOY (see MacFarlane 1989) calculate exactly the same average cross sections as FITACS from given average resonance

parameters. The differences can be kept small, however, with suitable energy-dependent parameters. Fig. 1 shows that this goal is achieved with the JEF-2 evaluation: The NJOY-generated average cross sections differ at most by about 1.5 percent from the FITACS-generated recommended values except above the second (4+) inelastic threshold at 149 keV where the ENDF restriction to one inelastic ("residual") width begins to hurt. The point cross sections and the average resonance parameters coexisting in the file are thus reasonably consistent. Nevertheless, as a matter of principle, and as indicated by a flag in the JEF-2 file, average resonance parameters are to be used solely for the calculation of self-shielding (Bondarenko) factors, or for the sampling of resonance ladders in Monte Carlo calculations, whereas average cross sections (for infinite dilution) are to be obtained by interpolation between the point cross sections given in the file.

3. Comparison with Recent Capture Data

After the JEF-2 evaluation of the ^{238}U neutron cross sections had been completed new capture yield data were reported by Macklin et al. (1988). These data show partially resolved resonance structure, and they are systematically higher than the JEF-2 average capture cross section, as Fig. 2 shows. Now the directly observable capture yield divided by the sample thickness cannot simply be equated to the capture cross section except in the limit of vanishing sample thickness. For practical sample thicknesses the yield is always affected by self-shielding and multiple scattering. One has

$$\langle y_\gamma \rangle = \left\langle \frac{1 - e^{-n\sigma}}{n\sigma} n\sigma_\gamma + y_{\gamma s} \right\rangle, \quad (1)$$

where y_γ is the capture yield, i. e. the probability that an incident neutron is captured in the sample, $y_{\gamma s}$ the multiple-scattering contribution, σ the (Doppler-broadened) total cross section, σ_γ the (Doppler-broadened) capture cross section, n the sample thickness in at./b, and the angular brackets denote resolution broadening, i. e. an average over incident energies involving very many resonances. The first term on the right, the first-collision yield, is the capture cross section times the sample thickness times a factor describing self-shielding. Self-shielding tends to lower the yield, multiple scattering tends to increase it. At low keV energies the two effects almost cancel, at higher energies there is a net enhancement.

The average capture yield is thus a functional of the total and capture cross sections, complicated by their correlated resonance structure and by multiple-collision events, with cross sections changing violently from collision to collision. An analytical calculation is possible only with drastic, hence dubious, approximations. On the other hand Monte Carlo techniques permit high accuracy both in the sampling of resonance cross sections and in the simulation of multiple-collision events leading to eventual capture.

An updated version of a Monte Carlo program (SESH, Fröhner 1968), written for the calculation of sample-thickness corrections to resonance-averaged data, was employed to calculate, from the JEF-2 average parameters, capture yields expected for the sample used by Macklin et al. The program simulates multiple-collision events, generating for each collision a "resonance environment" by sampling resonance spacings from the Wigner distribution and partial widths from Porter-Thomas distributions with the average spacings and average widths taken from the file. In this way a resonance ladder is generated whose length was taken as eight resonances, four to the left and four to the right of the energy

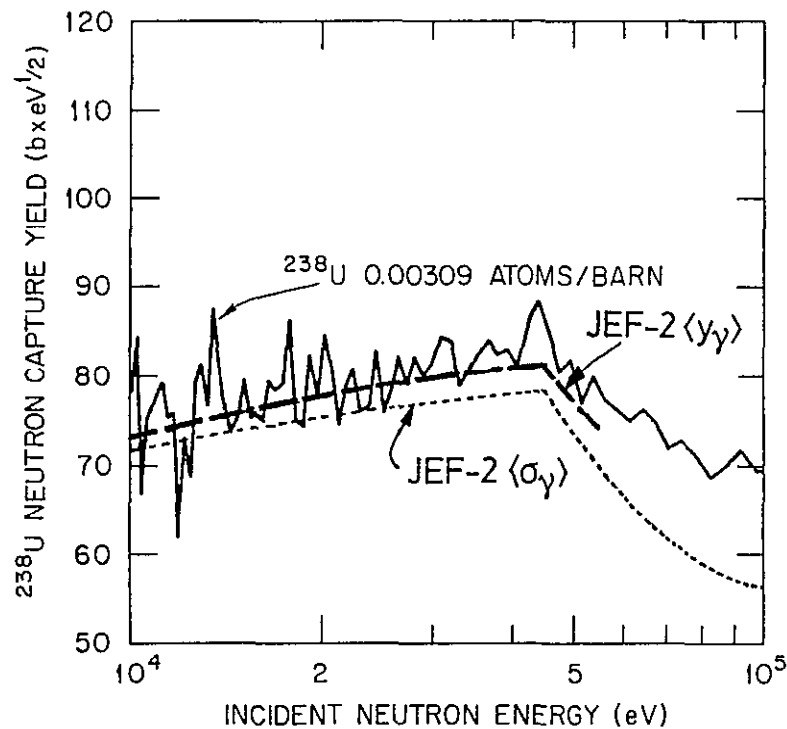


Fig. 2. High-resolution ORELA capture yields divided by sample thickness, i. e. raw capture cross sections uncorrected for resonance self-shielding and multiple scattering (fluctuating curve, from Macklin et al. 1988), recommended JEF-2 capture cross sections (dotted line), and capture yields calculated with Monte Carlo techniques from JEF-2 average resonance parameters (broken line), all multiplied by \sqrt{E} .

of interest. This is done for all level sequences (level spins and parities) excited by the s-, p- and d-wave. The Doppler-broadened cross section is then calculated from the sampled resonance parameters in single-level Breit-Wigner (SLBW) approximation at the energy of interest. The single-level approximation is adequate for a simulation of resonance effects in this energy range according to de Saussure and Perez (1973). The Monte-Carlo generated average cross sections are routinely checked against the analytical SLBW expressions to make sure they agree within sampling errors (less than 1 percent with the employed sample size of 100 000 per energy point). The calculated yield curve, shown as a broken line in Fig. 2, is reasonably consistent with the average of the observed fluctuating capture yields, at least below the Wigner cusp at the first inelastic (2+) threshold at 45 keV.

The relative shape of the evaluated average capture cross section is nicely confirmed below about 200 keV by a recent measurement with Fe and Si filtered neutron beams at 24, 55 and 146 keV reported by Kobayashi, Yamamoto and Fujita (1991).

A very accurate absolute capture cross section measurement was announced by Quang

and Knoll (1990). Using a calibrated spherical Sb-Be photo-neutron source and the manganese bath technique they obtained, essentially without reliance on any reference cross section,

$$\langle\sigma_{\gamma}\rangle = 494 \pm 11 \text{ mb} \quad \text{at } E = 23 \text{ keV}.$$

The JEF-2 value at the same neutron energy, 500 mb, is in excellent agreement with this precision measurement. That is a rather direct confirmation of the absolute value of the evaluated average capture cross section, at least at relatively low keV energies, yet it does not shed much light on the correctness of the resonance structure implied by the average resonance parameters in the file. The resonance structure, however, is decisive for self-shielding in bulk material, e. g. in fission reactor fuel or in breeder blankets.

4. Comparison with Thick-Sample Transmission Data

The representation of the resonance structure can be tested by comparing cross section functionals like thick-sample transmission or capture self-indication ratios computed from the evaluated file with resonance-averaged measurements of these quantities. The transmission of a "filter" sample of thickness n (nuclei/b), averaged over a suitably broad energy interval, can be written as

$$\langle e^{-n\sigma} \rangle = e^{-n\langle\sigma\rangle} \left(1 + \frac{n^2}{2} \text{var } \sigma + \dots \right), \quad (2)$$

where the variance, $\text{var } \sigma = \langle (\sigma - \langle\sigma\rangle)^2 \rangle = \langle\sigma^2\rangle - \langle\sigma\rangle^2$, and higher moments of the total cross section distribution indicate how pronounced the resonance structure is. The relevant parameters are the strength functions and distant-level parameters (or the effective nuclear radii). They determine, for the various partial waves, the ratio of compound (resonance) to direct (potential scattering) cross section. The thicker the sample, the more sensitive are the observed data to the cross section structure, the main weight being placed on the total cross section between resonances.

Resonance cross sections were again sampled with the SESH program and the corresponding transmissions averaged. The averages were then compared to the extensive transmission data base measured by Byoun et al. (1972), Bokhovko et al. (1988), and Grigoryev et al. (1990). Figs. 3 and 4 show a comparison with the most accurate measurements. The numbers plotted in Fig. 4 are shown in Table 1. Even for the thickest sample, corresponding to about 3 mean free paths, the calculated values are seen to agree well with the experimental data, usually within the error bars. (Monte Carlo sampling was performed again with 100 000 neutron histories per initial energy to keep sampling errors below 1 percent). Comparable agreement was found with the data of Grigoryev et al. (1990). Thus the structure of the total cross section appears to be well represented by the average resonance parameters given in the new evaluation.

5. Comparison with Measured Self-Indication Ratios

Capture self-indication ratios are obtained if the transmitted part of the neutron beam is permitted to undergo capture in a thin "indicator" sample (or "radiator") placed downstream of the filter sample, consisting of the same material, and viewed by gamma-ray detectors. From "filter in" and "filter out" runs one obtains the capture self-indication ratio, given by

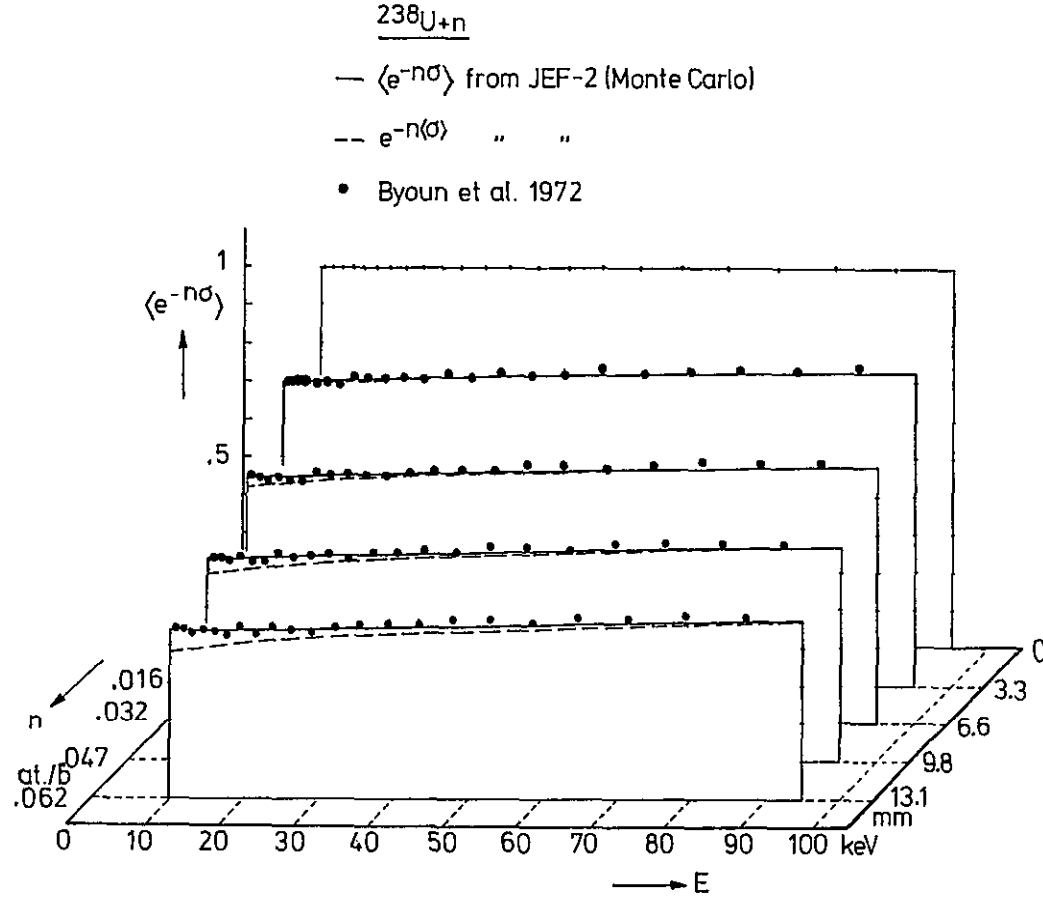


Fig. 3. Thick-sample transmission data of Byoun et al. (1972) (solid circles) and curves generated with Monte Carlo techniques from JEF-2 average resonance parameters (solid lines). Also shown are the transmission curves obtained without due account of resonance self-shielding (broken lines).

$$\frac{\langle e^{-n\sigma\sigma_\gamma} \rangle}{\langle \sigma_\gamma \rangle} = e^{-n\langle\sigma\rangle} \left(1 - n \frac{\text{cov}(\sigma, \sigma_\gamma)}{\langle \sigma_\gamma \rangle} + \dots \right), \quad (3)$$

at least for a very thin radiator sample. Practical samples are not ideally thin, however, so the capture cross section σ_γ in this expression ought to be replaced by the capture yield y_γ that includes self-shielding and multiple-collision capture. In any case the self-indication ratio depends on the total and the relative capture cross sections and on their correlated resonance structure given by the covariance, $\text{cov}(\sigma, \sigma_\gamma) = \langle (\sigma - \langle\sigma\rangle)(\sigma_\gamma - \langle\sigma_\gamma\rangle) \rangle =$

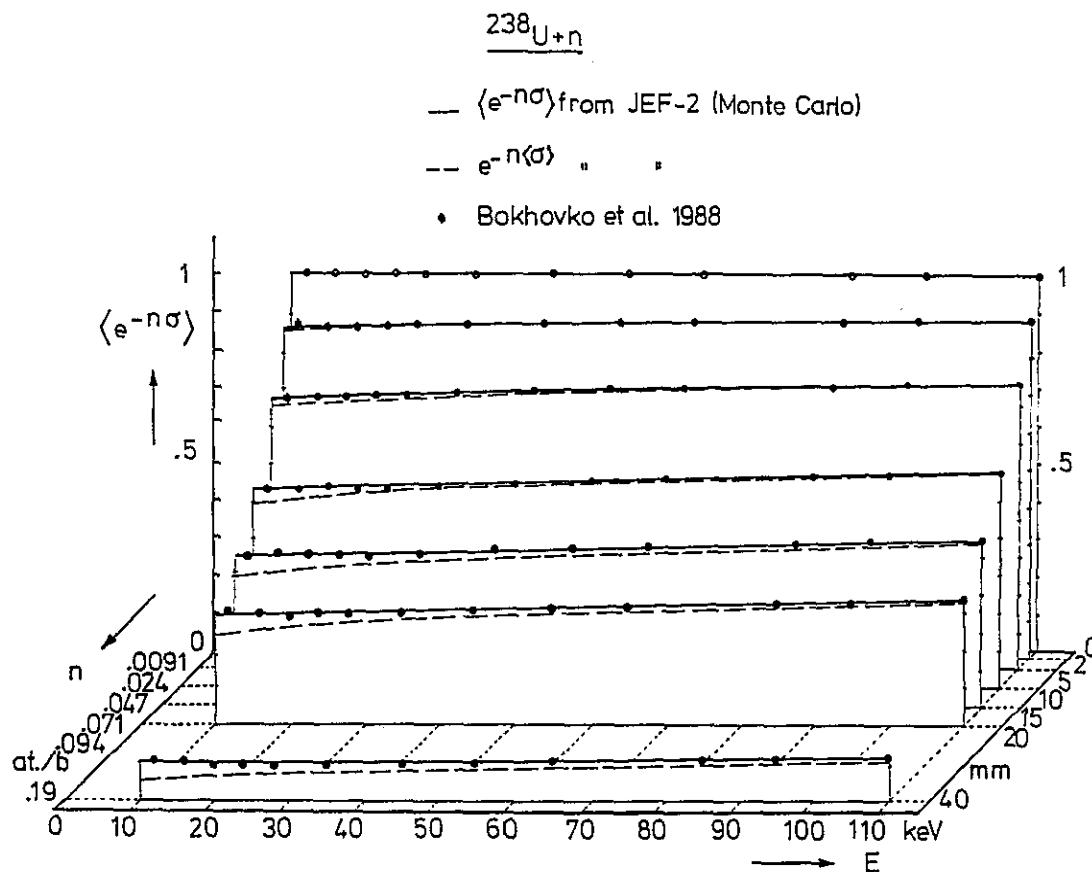


Fig. 4. Thick-sample transmission data of Bokhovko et al. (1988) (solid circles) and curves generated with Monte Carlo techniques from JEF-2 average resonance parameters (solid lines). Also shown are the transmission curves obtained without due account of resonance self-shielding (broken lines). Most error bars are slightly smaller than the point symbols.

$\langle \sigma \sigma_\gamma \rangle - \langle \sigma \rangle \langle \sigma_\gamma \rangle$, and by higher mixed moments of the total and the capture cross section distributions. As in transmission measurements the accuracy is inherently high since corrections to numerator and denominator tend to cancel at least partially, and the flux calibration and capture detector efficiency factors cancel exactly. The main weight is placed, however, on the peak regions, not on the regions between the peaks as in transmission data, since self-indication ratios are essentially capture-weighted transmissions, and capture peaks coincide with transmission dips.

The SESH code was used again to calculate the observable ratio, $\langle e^{-n\sigma} y_\gamma \rangle / \langle y_\gamma \rangle$, from JEF-2 average resonance parameters. The results were compared with the data of Byoun et al. (1972), Bokhovko et al. (1988), and Grigoryev et al. (1990). None of these authors discusses sample thickness effects, i.e. the difference between capture cross section and

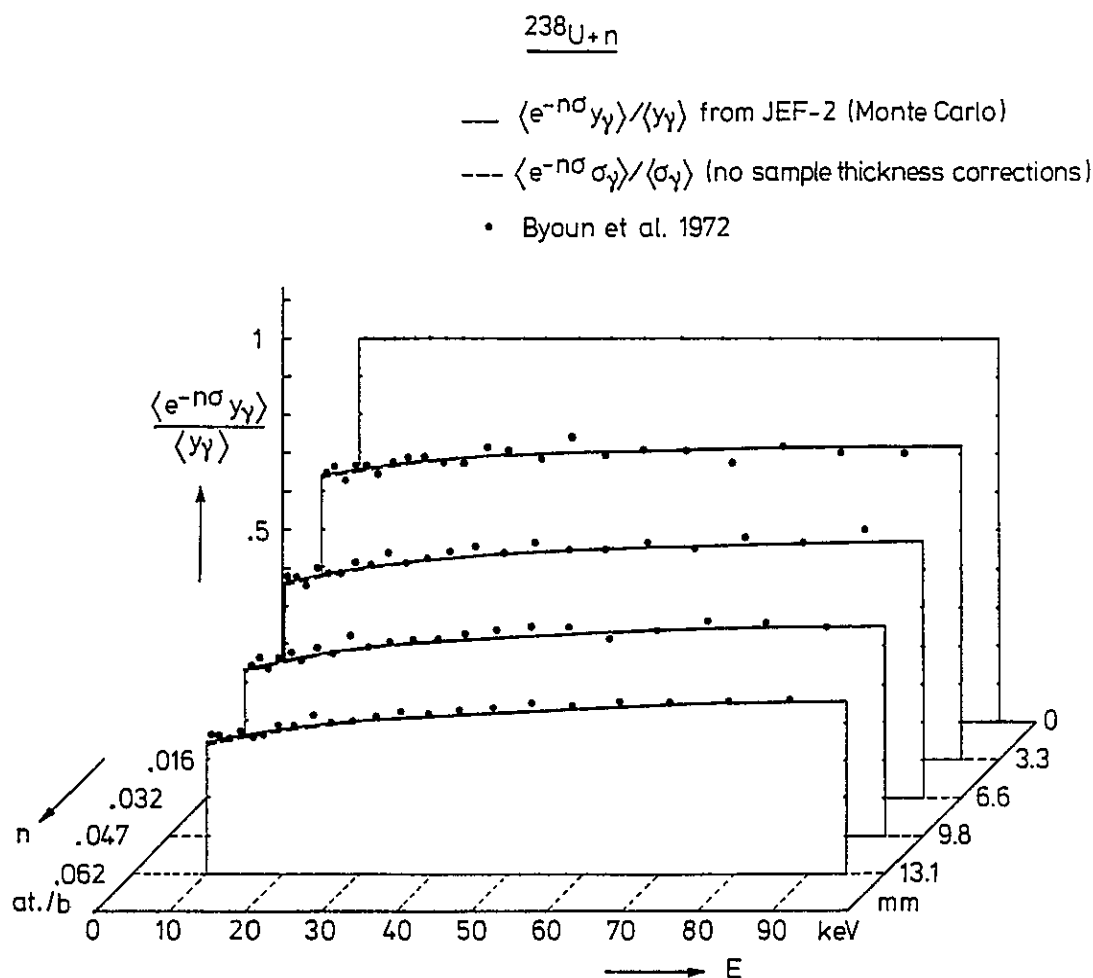


Fig. 5. Self-indication ratios measured by Byoun et al. (1972) (solid circles) and curves generated with Monte Carlo techniques from JEF-2 average resonance parameters (solid lines). Also shown are the results obtained without account for resonance self-shielding and multiple-collision capture, i. e. for vanishing radiator sample thickness (broken lines). The actual radiator sample thickness was 0.00376 at./b.

capture yield, although the corrections are not negligible for the radiator samples used in the experiments. It is true that the corrections to numerator and denominator largely cancel, yet there is a net effect of a few percent at low energies. Figs. 5 and 6 show the comparison of calculated and measured self-indication ratios, the latter being assumed as uncorrected for sample thickness effects. A subset of the numbers plotted in Fig. 6 is shown in Table 2. Agreement is seen to be quite good, in particular with the very accurate data of Bokhovko et al. (1988), and the same is true for the data of Grigoryev et al. (1990). It is evident that not only the structure of the total cross section but also that of the capture cross section is well represented by the average resonance parameters given in the new ^{238}U evaluation.

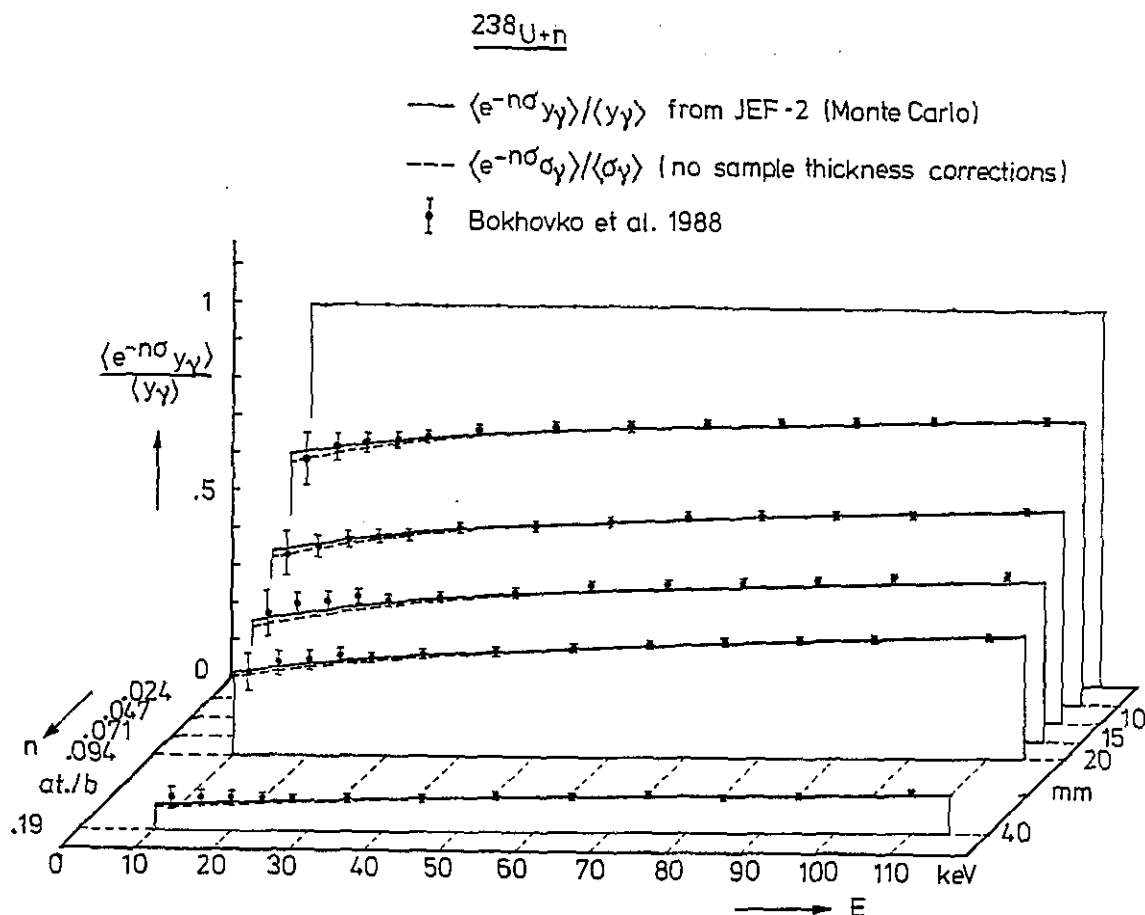


Fig. 6. Self-indication ratios measured by Bokhovko et al. (1988) (solid circles) and curves generated with Monte Carlo techniques from JEF-2 average resonance parameters (solid lines). Also shown are the results obtained without account for resonance self-shielding and multiple-collision capture, i. e. for vanishing radiator sample thickness (broken lines). The actual radiator sample thickness was 0.00646 at./b.

6. Summary and Conclusions

Comparison of the newly evaluated average ^{238}U (n, γ) cross sections in the unresolved resonance region with recent capture yield data of Macklin et al. (1988) shows reasonable agreement if due account is taken of self-shielding and multiple-collision capture. A new absolute precision result, $\langle \sigma_\gamma \rangle = 496 \pm 11$ mb at 23 keV (Quang and Knoll 1990) is in perfect agreement with the recommended value $\langle \sigma_\gamma \rangle = 500$ mb at that energy in the new JEF-2 evaluation.

Monte-Carlo generated average transmission values and self-indication ratios agree well with the extensive experimental data base provided by Byoun et al. (1972), Bokhovko et al. (1988), and Grigoryev et al. (1990). The agreement indicates that not only the absolute

total and capture cross sections recommended in the JEF-2 evaluation are realistic but also the average resonance parameters specifying the resonance structure.

In order to see the consequences for self-shielding calculations let us consider the relationship between self-shielding (Bondarenko) factors on one hand and average transmission values and self-indication ratios on the other,

$$f_7 = \frac{\langle \sigma_7 / (\sigma + \sigma_d) \rangle}{\langle \sigma_7 \rangle \langle 1 / (\sigma + \sigma_d) \rangle} = \frac{\int_0^\infty dn e^{-n\sigma_d} \langle e^{-n\sigma} \sigma_7 \rangle / \langle \sigma_7 \rangle}{\int_0^\infty dn e^{-n\sigma_d} \langle e^{-n\sigma} \rangle}, \quad (4)$$

where σ_d is the (constant) dilution cross section and $\langle \dots \rangle$ denotes group averages. It is obvious that the possibility to predict $\langle e^{-n\sigma} \rangle$ and $\langle e^{-n\sigma} \sigma_7 \rangle / \langle \sigma_7 \rangle$ in a reliable way means that one can also predict f_7 reliably. The present results indicate that the new ^{238}U evaluation allows prediction of average transmission and self-indication ratios at room temperature with an accuracy of 1-3 percent in the range of sample thicknesses n covered by the data (down to about 10 percent transmission corresponding to more than two mean free paths). Because of the positive correlation between numerator and denominator in Eq. 4 it may thus be expected that self-shielding factors can be computed with an accuracy of 0.5-1.5 percent. At elevated temperatures the resonance structure is less pronounced due to Doppler broadening so that self-shielding factors differ less from unity. They may therefore be expected to remain at least equally accurate also at higher temperatures.

The JEF-2 capture cross sections in the unresolved resonance range, based on microscopic data including resolved resonance parameters and on Hauser-Feshbach theory, agree very well with those evaluated pointwise by Poenitz (1988) for the ENDF/B-VI standards file, with the JENDL-3 evaluation that relies heavily on reactor experiments (Kanda et al. 1991), and with a new BROND evaluation (Blokhin et al. 1991). The mutual deviations below 200 keV are less than 1.5 percent, indicating that the (infinite-dilution) average capture cross section of ^{238}U may now be known to about 1 - 2 percent between 10 and 200 keV. This comes close to the accuracies requested for nuclear technology and, in particular, for nuclear reactor safety research.

ACKNOWLEDGMENTS. It is a pleasure to thank Dr. N.B. Yaneva (Sofia, Bulgaria) for early communication of experimental results, and Mrs. B. Krieg and Dr. I. Broeders for help with the NJOY calculations. Support by the German Safety Research Project and by Prof. G. Kessler and Dr. H. Küsters is acknowledged.

Table 1. Thick-sample transmissions and uncertainties of Bokhovko et al. (1988) compared with Monte Carlo results based on JEF-2, as plotted in Fig. 4.

E (keV)	Sample Thicknesses (at./b)					
	0.0091 (2 mm)	0.0237 (5 mm)	0.0474 (10 mm)	0.0707 (15 mm)	0.0943 (20 mm)	0.19 (40 mm)
10-14	0.884 ± 0.006	0.718 ± 0.005	0.525 ± 0.009	0.398 ± 0.008	0.299 ± 0.005	0.104 ± 0.005
	0.875	0.717	0.526	0.396	0.296	0.100
14-18	0.876 ± 0.006	0.717 ± 0.004	0.523 ± 0.007	0.405 ± 0.007	0.296 ± 0.003	0.102 ± 0.004
	0.878	0.719	0.532	0.398	0.295	0.099
18-22	0.880 ± 0.004	0.719 ± 0.004	0.531 ± 0.006	0.400 ± 0.005	0.288 ± 0.002	0.093 ± 0.003
	0.880	0.723	0.535	0.399	0.296	0.098
22-26	0.881 ± 0.004	0.724 ± 0.003	0.527 ± 0.005	0.402 ± 0.004	0.295 ± 0.002	0.094 ± 0.002
	0.882	0.725	0.535	0.401	0.296	0.097
26-30	0.881 ± 0.004	0.722 ± 0.003	0.527 ± 0.006	0.398 ± 0.004	0.292 ± 0.002	0.093 ± 0.002
	0.883	0.728	0.537	0.403	0.296	0.097
30-40	0.883 ± 0.004	0.731 ± 0.003	0.536 ± 0.005	0.408 ± 0.004	0.298 ± 0.002	0.095 ± 0.002
	0.885	0.732	0.541	0.407	0.301	0.098
40-50	0.887 ± 0.004	0.739 ± 0.003	0.540 ± 0.004	0.417 ± 0.004	0.304 ± 0.002	0.099 ± 0.002
	0.888	0.736	0.546	0.410	0.305	0.099
50-60	0.887 ± 0.004	0.743 ± 0.003	0.549 ± 0.004	0.420 ± 0.004	0.308 ± 0.002	0.100 ± 0.002
	0.890	0.740	0.551	0.416	0.309	0.101
60-70	0.893 ± 0.004	0.748 ± 0.003	0.554 ± 0.004	0.425 ± 0.004	0.316 ± 0.002	0.103 ± 0.002
	0.891	0.743	0.556	0.420	0.314	0.103
80-90	0.896 ± 0.004	0.751 ± 0.003	0.563 ± 0.004	0.435 ± 0.004	0.324 ± 0.002	0.108 ± 0.002
	0.894	0.749	0.564	0.429	0.322	0.108
90-100	0.899 ± 0.004	0.757 ± 0.003	0.565 ± 0.003	0.440 ± 0.003	0.328 ± 0.002	0.110 ± 0.002
	0.896	0.752	0.568	0.433	0.327	0.110
100-120	0.904 ± 0.004	0.760 ± 0.003	0.573 ± 0.003	0.447 ± 0.003	0.337 ± 0.002	0.114 ± 0.002
	0.898	0.756	0.574	0.439	0.333	0.114

Note: The interval 70-80 keV is missing from the table given by Bokhovko et al. (1988)

Table 2. Self-indication ratios and uncertainties of Bokhovko et al. (1988) compared with Monte Carlo results based on JEF-2, as plotted in Fig. 6.

E (keV)	Sample Thicknesses (at./b)				
	0.0237 (5 mm)	0.0474 (10 mm)	0.0707 (15 mm)	0.0943 (20 mm)	0.19 (40 mm)
10-14	0.641 ± 0.069	0.438 ± 0.060	0.329 ± 0.060	0.221 ± 0.049	0.084 ± 0.030
	0.654	0.455	0.317	0.229	0.065
18-22	0.683 ± 0.025	0.477 ± 0.021	0.363 ± 0.024	0.254 ± 0.025	0.085 ± 0.017
	0.682	0.478	0.342	0.245	0.070
26-30	0.698 ± 0.016	0.488 ± 0.014	0.365 ± 0.015	0.261 ± 0.012	0.083 ± 0.012
	0.696	0.495	0.357	0.260	0.076
40-50	0.726 ± 0.014	0.511 ± 0.012	0.390 ± 0.011	0.279 ± 0.010	0.084 ± 0.010
	0.716	0.519	0.381	0.280	0.084
60-70	0.738 ± 0.011	0.541 ± 0.012	0.412 ± 0.011	0.301 ± 0.008	0.093 ± 0.007
	0.728	0.538	0.400	0.295	0.092
80-90	0.745 ± 0.010	0.544 ± 0.009	0.422 ± 0.009	0.316 ± 0.008	0.094 ± 0.006
	0.736	0.549	0.415	0.309	0.098
100-120	0.753 ± 0.008	0.562 ± 0.007	0.443 ± 0.008	0.327 ± 0.007	0.109 ± 0.006
	0.751	0.565	0.431	0.324	0.102

REFERENCES

- A.I. Blokhin, A.V. Ignatyuk, B.D. Kuzminov, V.N. Manokhin, G.N. Manturov and M.N. Nikolaev, Proc. Internat. Conf. on Nucl. Data in Sci. and Technology, Jülich, 1991 (in print); B.D. Kuzminov, private communication (1991)
- M.V. Bokhovko, V.N. Kononov, G.N. Manturov, E.D. Poletaev, V.V. Sinitsa and A.A. Voevodskij, Yad. Konst. 3 (1988) 11; Engl. transl. INDC(CCP)-322 (1990) p. 5
- T.Y. Byoun, R.C. Block and T. Semler, Proc. Kiamesha Lake Conf. 1972, CONF-720901, Book 2, p. 1115 (1972)
- G. de Saussure and R.B. Perez, Nucl. Sci. Eng. 52 (1973) 382
- F.H. Fröhner, Report GA-8380 (1968)
- F.H. Fröhner, Nucl. Sci. Eng. 102 (1989) 119
- Yu.V. Grigoriev, V.N. Koshcheev, G.N. Manturov, I.A. Sirakov, V.V. Sinitsa, N.B. Yaneva Obninsk report FEI-2072 (1990)
- Y. Kanda, Y. Kikuchi, Y. Nakajima, M.G. Sowerby, M.C. Moxon, F.H. Fröhner, W.P. Poenitz and L.W. Weston, Proc. Internat. Conf. on Nucl. Data in Sci. and Technology, Jülich, 1991 (in print)
- K. Kobayashi, S. Yamamoto and Y. Fujita, Proc. Internat. Conf. on Nucl. Data in Sci. and Technology, Jülich, 1991 (in print)
- B.D. Kuzminov, private communication (1991)
- R.E. MacFarlane, Proc. Seminar on NJOY and Themis, OECD Paris (1989) p. 7
- Roger L. Macklin, R.B. Perez, G. de Saussure and R.W. Ingle, Proc. Int. Conf. Nucl. Data for Sci. and Technol., Mito 1988, ed. S. Igarasi, Tokyo (1988) p. 75
- M. Moxon, M. Sowerby, Y. Nakajima and C. Nordborg, Proc. Internat. Reactor Physics Conf., Jackson Hole, ANS (1988), vol. I, p. 281
- W.P. Poenitz, private communication (1988)
- E. Quang and G. Knoll, Prog. Rept. BNL-NCS-44362 (1990) p. 112